NMR studies of ordered structures and valence states in the successive valence-transition system EuPtP

T. Mito,[1,*] K. Nishitani,[1] T. Koyama,[1] H. Muta,[1] T. Maruyama,[1] G. Pristáš,[1] K. Ueda,[1] T. Kohara,[1] A. Mitsuda,[2] M. Sugishima,[2] and H. Wada[2]

[1]*Graduate School of Material Science, University of Hyogo, Hyogo 678-1297, Japan*

[2]*Department of Physics, Kyushu University, Fukuoka 812-8581, Japan*

(Received 9 May 2014; revised manuscript received 6 October 2014; published 4 November 2014)

We have studied EuPtP, which undergoes two successive valence transitions at $T_A \sim 240$ K and $T_B \sim 200$ K by ^{31}P-nuclear magnetic resonance (NMR) measurements. From the analysis of NMR spectra, we obtained plausible ordered structures and Eu valence states in three phases divided by T_A and T_B. These ordered structures well explain observed inequivalent P sites and the intensity ratio of the NMR spectra arising from these P sites. The results are also in good accordance with mean Eu valence measured by the x-ray absorption spectroscopy. We also discuss Eu $4f$ states and the origin of the transitions from the measurements of nuclear spin lattice relaxation rate and hyperfine coupling constant.

DOI: 10.1103/PhysRevB.90.195106 PACS number(s): 71.27.+a, 75.20.Hr, 75.30.Mb, 76.60.−k

I. INTRODUCTION

The interplay between the valence of lanthanide ions and a great variety of features observed in lanthanide compounds is one of central issues in the study of f electron systems. Many lanthanide-based heavy fermion systems show an intermediate valence state: the valence of the lanthanides deviates from an integer due to the underlying hybridization between conduction and f electrons (c-f hybridization). Normally, the intermediate valence gradually changes as functions of experimental parameters, including temperature, pressure, and magnetic field. However, some of lanthanide compounds exhibit a sudden valence change, so called valence transition. The valence change in Ce-, Sm-, Eu-, and Yb-based compounds influences the entire physical properties of them, because it involves changes of not only electric properties but also magnetic properties: one of their divalent and trivalent states (trivalent and tetravalent states for Ce) is magnetic, and the other is nonmagnetic (total angular momentum $J = 0$).

In the Ce- and Yb-based systems, only a few compounds are known for their valence transitions, for example, Ce metal [1] and $YbInCu_4$ [2,3]. On the other hand, the valence transition is seen in a relatively larger number of Eu-based compounds [4]. The origin of this tendency is still an open question. To solve the mechanism of the valence transition in each Eu-based material and to clarify characteristics of Eu-4f states, it is indispensable to accumulate studies from the microscopic point of view. Nevertheless, there are few reports of nuclear magnetic resonance (NMR) study investigating the valence transition or even paramagnetic states in the Eu-based compounds. This may be because fluctuations of large magnetic moments in Eu^{2+} state ($S = J = 7/2$, effective moment $\mu_{eff} = 7.94\mu_B$) lead to difficulties in observing NMR signals.

Among the Eu-based valence transition compounds, EuPtP is one of rare materials that show two valence transitions as a function of temperature. At high temperatures above $T_A \sim 240$ K, EuPtP basically crystallizes in the hexagonal Ni_2In-type structure where Eu and Pt-P layers alternately stack along the c axis (see the inset of Fig. 1). There is only one Eu site for $T > T_A$, while this compound undergoes first-order phase transitions at T_A and $T_B \sim 200$ K, resulting in the existence of inequivalent Eu sites at low temperatures. The drops of the susceptibility and of the unit cell volume both just below T_A and T_B are consistent with an increase in Eu^{3+} component [5,6]: Eu^{3+} state is nonmagnetic, and the lattice generally shrinks with smaller Eu^{3+} ions than Eu^{2+} ions. Indeed, the reports of the Eu L_{III} edge x-ray absorption spectroscopy (XAS) indicate that the Eu valence changes at T_A and T_B [7,9], that is, the mean values are estimated as 2.10 for $T > T_A$ (denoted as α phase), 2.33 for $T_B < T < T_A$ (β phase), and 2.41 for $T < T_B$ (γ phase) [9]. Moreover, EuPtP exhibits antiferromagnetic ordering at 8.6 K [5,7,8].

There are also several works which attempted to identify ordered structures in the β and γ phases [7,9]. However, this issue has not been fully confirmed yet. One of the points is that experimentally measured mean Eu valences deviate from values expected for structural candidates, especially in the α and γ phases. Moreover, it is still controversial whether the Eu ions in the α phase is in the intermediate valence state or in the divalent state. We have therefore carried out ^{31}P-NMR measurements on EuPtP to clarify these problems. Taking advantages of probing ^{31}P nucleus, which is known as one of nuclides giving strong NMR signals (natural abundance 100 %, gyromagnetic ratio $\gamma_n/2\pi = 17.237$ MHz/T) and of using a 15 T magnet, we could observe NMR signals in the paramagnetic state of this compound. Although ^{31}P nucleus (nuclear spin $I = 1/2$ and no nuclear quadrupole moment) does not directly couple to the Eu valence, the opposite magnetic character of the Eu^{3+} and Eu^{2+} states allows us to get information on $4f$ electron configurations at neighboring Eu sites by measuring the Knight shift.

From the present studies, we obtained plausible ordered structures in the β and γ phases, and no indication of valence fluctuation was found in the α phase. The results reasonably explain the mean Eu valence determined by other experiments. Eu moments are well localized in the all phases, indicating small c-f hybridizations. No development of magnetic correlations was observed as approaching the valence transition

*mito@sci.u-hyogo.ac.jp

temperatures, suggesting that the mechanism of the transitions is of purely electric origin or possibly associated with Fermi surface properties for the appearance of the β phase.

II. EXPERIMENTAL DETAILS

Single crystals of EuPtP were grown by a Pb-flux method [6,10]. We used a powdered sample for the NMR measurements. The ^{31}P-NMR measurements were performed using a standard spin-echo technique with a phase-coherent pulsed spectrometer. NMR spectra were obtained at a fixed frequency of 172.3 MHz and by sweeping magnetic field with a commercial 15 T superconducting magnet. Nuclear spin relaxation time T_1 was measured by a single rf-pulse saturation method. The susceptibility of a single crystal was measured using a superconducting quantum interference device (SQUID) at the maximum magnetic field (7 T) in order to compare it with the NMR data.

III. RESULTS AND DISCUSSION

A. ^{31}P-NMR spectra

Figure 1 shows the temperature dependence of ^{31}P-NMR lines in the temperature range from 30 to 300 K. Two and three well-identified lines are observed above T_B (α and β phases) and below T_B (γ phase), respectively. All of the resonance lines can be fitted by a Lorentzian function, and the spectra are entirely different from a conventional powder pattern. Therefore the obtained line shape implies that the grains of the powder sample orient along the magnetic field due to the anisotropic magnetization, so that the c axis is perpendicular to the fields (the easy axis is perpendicular to the c axis [6]). The temperature dependence of the Knight shift estimated from the resonance fields will be shown later.

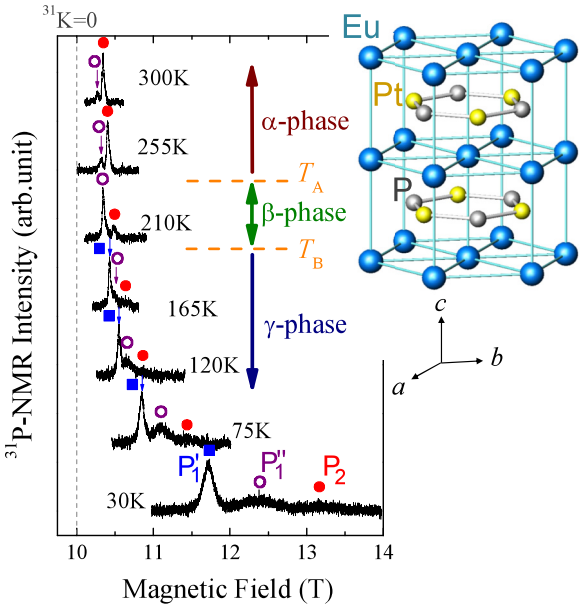

FIG. 1. (Color online) ^{31}P-NMR spectra measured at different temperatures from 30 to 300 K. The dotted line indicates a field of $K = 0$. The basic crystal structure in the α phase of EuPtP is also illustrated.

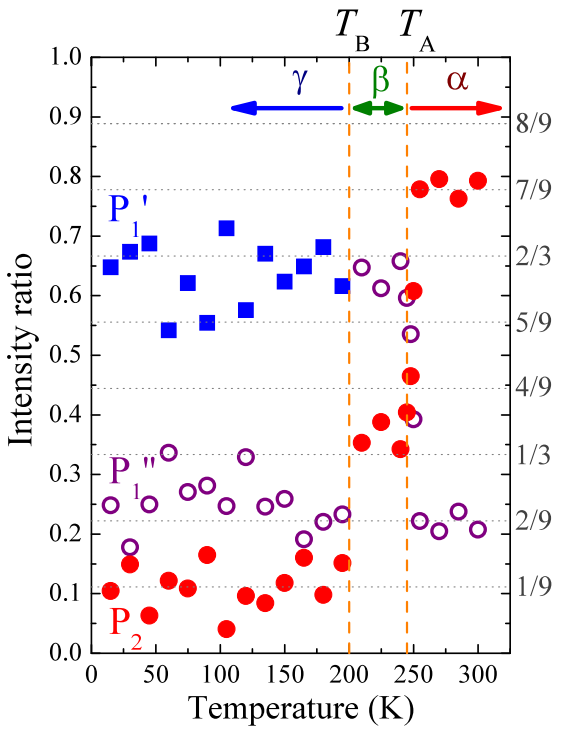

FIG. 2. (Color online) The intensity ratio of the signal P'_1, P''_1, and P_2 measured at different temperatures. See text for details.

In Fig. 2, we show the intensity ratio of these resonance lines at different temperatures. Here, the integral intensity was corrected by using transverse relaxation time T_2 data. The intensity of the ^{31}P-NMR line is proportional to the number of P atoms occupying the same site in the unit cell. Therefore, from the number of resonance lines (namely, the number of inequivalent P sites) and their intensity ratio, one can estimate the ordered structures in the three phases. Moreover, we can extract information on the local Eu valence by comparing the present structural models to the Eu mean valence measured by other experiments. Hereafter, we will discuss possible ordered structures on the assumption that the hexagonal structure is maintained in the all phases, because there is no experimental evidence for the breakdown of this symmetry so far. First, we start from the results on the β phase in which the ordered structure is already almost identified.

Figure 3(a) shows the detailed ^{31}P-NMR spectra in the β phase. The observation of two different resonance lines indicates the presence of two inequivalent P sites. These two sites are hereafter denoted as P_1 (lower resonance field) and P_2. The intensity ratio of the signals P_1 and P_2 is approximately 2 : 1 as shown in Fig. 2. These experimental results are well explained within a model where Eu^{2+} and Eu^{3+} basal planes stack along the c axis in order of Eu^{2+}-Eu^{2+}-Eu^{3+}-Eu^{2+}-Eu^{2+}-Eu^{3+}-$\cdots$. Then, the numbers of P_1 atoms (between Eu^{2+} and Eu^{3+} planes) and P_2 atoms (between Eu^{2+} planes) is 2 : 1, as illustrated in Fig. 3(b). This arrangement of the Eu^{2+} and Eu^{3+} layers is in good agreement with the periodicity suggested from a resonant x-ray diffraction measurement [9]. We therefore conclude that the present interpretation for the β phase is most probable, and we proceed to deduce the ordered structures for other phases in the similar manner.

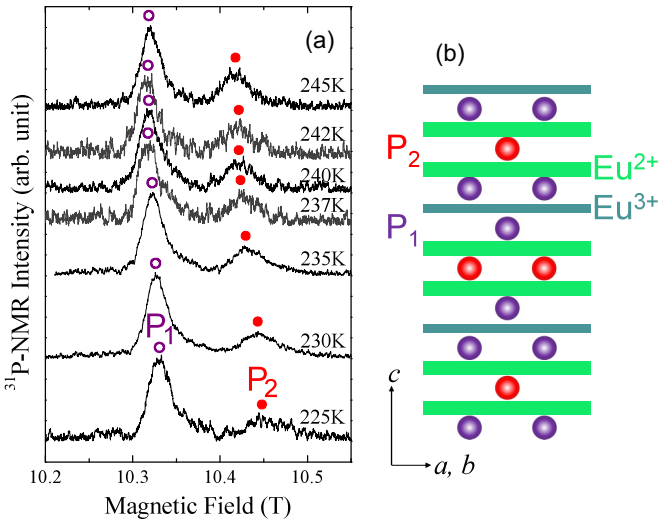

FIG. 3. (Color online) (a) Temperature dependence of ^{31}P-NMR spectra in the β phase, for $225 < T < 245$ K. (b) The model of ordered structure in the β phase. The thicker and thinner horizontal lines indicate the basal layers consisting of Eu^{2+} and Eu^{3+} ions, respectively. The Pt atoms are omitted for simplicity.

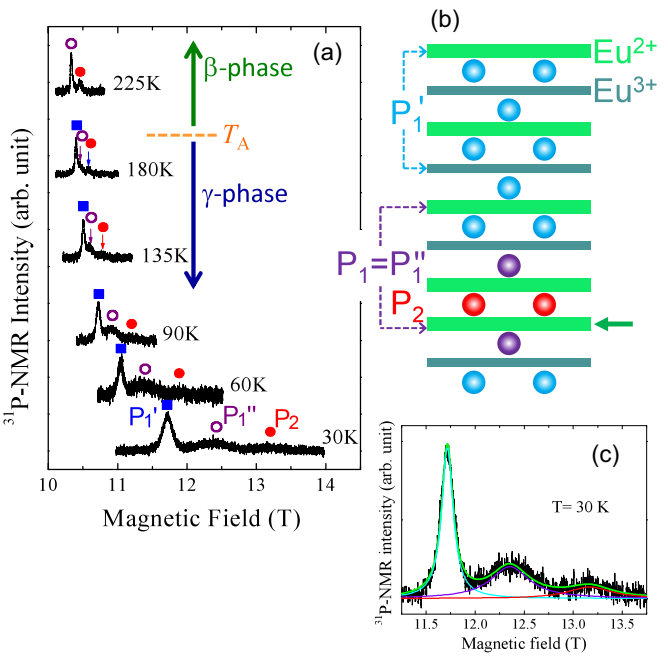

FIG. 4. (Color online) (a) Temperature dependence of ^{31}P-NMR spectra below 225 K, mainly in the γ phase. (b) The model of ordered structure in the γ phase obtained from the present measurement. The dotted arrows indicate the second nearest-neighbor Eu layers of the P_1' and P_1 sites. Approximately, 1/9 Eu layers irregularly orders as indicated by the solid arrow. (c) ^{31}P-NMR spectrum at 30 K. The solid lines are Lorentzian fits to the data by assuming the intensity ratio $P_1' : P_1''(= P_1) : P_2 = 6 : 2 : 1$ on the basis of the model illustrated in (b). The light blue, purple, and red lines correspond to P_1', $P_1''(= P_1)$, and P_2 sites, respectively. See text for details.

For the γ phase, three resonance lines are observed as shown in Fig. 4(a). Here, the two resonance lines at lower fields [denoted as P_1' and P_1'' in Fig. 4(a)] are originally split from the P_1 signal in the β phase, as the γ phase develops upon cooling. The P_1' and P_1'' atoms are therefore supposed to be placed in a similar environment to that of the P_1 sites, namely they are in between the Eu^{2+} and Eu^{3+} layers. Another point is that the small intensity of the P_2 signal is still observed in the γ phase. A model satisfying these experimental observations is illustrated in Fig. 4(b). Although the γ phase is basically dominated by a structure where the Eu^{2+} and Eu^{3+} layers alternately stack along the c axis, a small amount of the β phase persists down to the lowest temperature. One sees that both P_1' and P_1'' atoms sit between the Eu^{2+} and Eu^{3+} layers as indicated in Fig. 4(b). However, one of the two second nearest-neighbor Eu layers of the P_1' site consists of nonmagnetic Eu^{3+}, while both of those for the P_1'' site are magnetic Eu^{2+}. In this context, the surroundings of the P_1'' site corresponds to the P_1 site in the β phase. The ratio of such an irregularly ordered Eu layer is estimated to be $\sim 1/9$ from the observed intensity ratio (see Fig. 2), i.e., $P_1' : P_1''(= P_1) : P_2 \approx 6 : 2 : 1$ [see Fig. 4(c)]. The mean Eu valence expected from the present model (2.44) is in good agreement with 2.47 indicated from the XAS measurement [9].

As for the α phase, two resonance lines are observed as shown in Fig. 5(a), which is similar to in the β phase. Actually, when increasing temperature from the β phase to the α phase, the signals P_1 and P_2 do not show any significant changes in their resonance fields as shown in Fig 5(b). This indicates that the two P sites in the α phase are almost in the same surroundings with those in the β phase. However, in the α phase, the P_2 signal becomes stronger than P_1, implying obviously that the Eu^{2+} component is enhanced. On the other hand, the weak but certainly remaining P_1 signal suggests the persistence of a small amount of the β phase at least up to 300 K. An ordered structure which reproduces the present observations is illustrated in Fig. 5(c). From the intensity ratio of approximately $P_1 : P_2 = 2 : 7$ in the α phase, most of the Eu layers consist of Eu^{2+}, and about 10% of the Eu layers are trivalent. A resultant mean valence is 2.11, again in good agreement with the estimated value from the XAS measurement [9]. Note that the mean valence is static on the NMR time scale, implying that the 10% residual phase is segregated from the α phase and no indication of valence fluctuations was obtained from the present study.

We briefly comment on the first-order character of the transition at T_A. From the previous measurements of the macroscopic susceptibility, the large thermal hysteresis arising from the first-order nature is found at T_B but it is hardly observed at T_A [5,6]. Similarly, the hysteretic behavior is not clear in the temperature dependence of ^{31}P NMR lines around T_A as shown in Fig. 5(b), except for a small deviation between two spectra at 243 K, which is perhaps attributed to a small hysteresis. However, as temperature decreases across T_A, the spectral weight of the P_2 site is suddenly transferred to the P_1 without showing any intermediate state, and vice versa with increasing temperature. This is an unambiguous experimental evidence reflecting the first-order nature of the transition at T_A.

We here summarize the plausible ordered structure and Eu valence state in each phase as follows. The intrinsic structure of the α phase consists of Eu^{2+} ions. In the β phase, the Eu basal

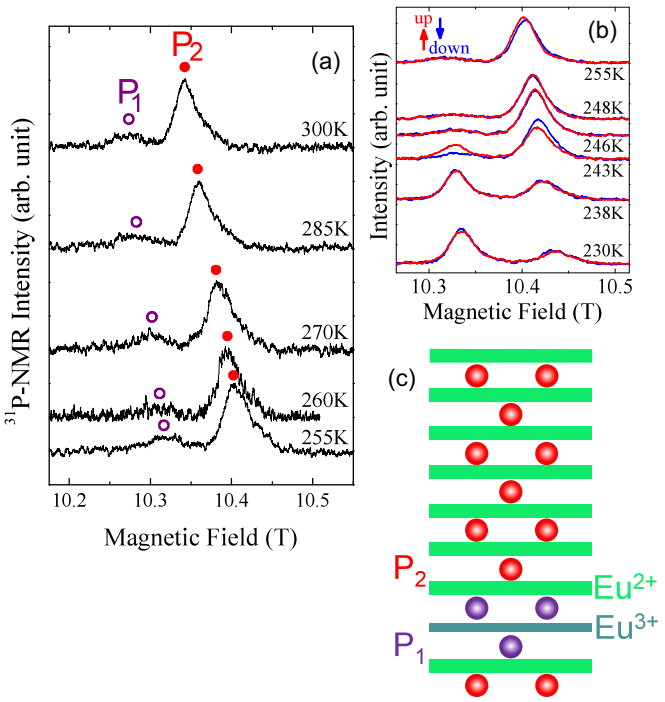

FIG. 5. (Color online) (a) Temperature dependence of ^{31}P-NMR spectra in the α phase. (b) ^{31}P-NMR spectra measured with increasing (red) and decreasing (blue) temperature across T_A. (c) The model of ordered structure in the α phase obtained from the present measurement.

planes stack along the c axis in order of Eu^{2+}-Eu^{2+}-Eu^{3+}-$\cdots$. For the γ phase, Eu^{2+} and Eu^{3+} basal planes alternately stack along the c axis. These ordered structures are entirely consistent with the result from the XAS measurement [9]. All of the structures consist of ferro-type charge order within a Eu layer, and we did not find any realistic model with antiferro-type order within the Eu layer to explain satisfactorily the observed NMR results. The indication of residual phases well accounts for why the experimentally determined mean valences deviate from the ideal values for the intrinsic ordered structures. The appearances of the residual β phase in the α and γ phases may be associated with the first-order nature of the transitions at T_A and T_B. Otherwise, possibly they are attributed to some kind of layered defects which are fixed to the β phase even though the system enters into other phases. This is suggested from the fact that the ratio of the irregularly ordered Eu layers is about 1/9, which is almost the same both in the α and γ phases. Such a layered defect might arise from surface effects. To elucidate their origin, a comparison between samples with different qualities will be useful.

B. Nuclear spin relaxation rate

The temperature dependence of $1/T_1$ provides information on Eu spin states. Figure 6 shows representative T_1 recovery curves for the P_1', P_1, and P_2 site. The data are quite well fitted by a single exponential function, which is a theoretically expected one for $I = 1/2$ systems, implying that each site consists of a single phase.

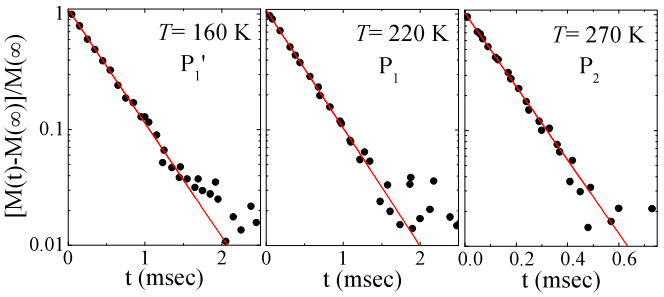

FIG. 6. (Color online) Representative T_1 recovery curves for the P_1' site ($T = 160$ K, left), the P_1 site ($T = 220$ K, middle), and the P_2 site ($T = 270$ K). $[M(\infty) - M(\infty)]/M(\infty)$ are plotted against time t, where $M(t)$ is the nuclear magnetization at t. Solid lines are single exponential fits to the data.

In Fig. 7(a), we plot $1/T_1$ measured at the signals P_1' (γ phase), P_1 (β phase), and P_2 (α phase), all of which arise from the intrinsic sites in these phases. For the P_2 site, we could not obtain reliable data below T_A due to too weak signal intensity. The T_1 relaxation in a localized f-electron system is generally expressed as a combination of two contributions; one is a relaxation due to the magnetic fluctuations of local moments and the other is a Korringa-type contribution from the conduction electrons, then

$$1/T_1 = (1/T_1)_f + (1/T_1)_c. \quad (1)$$

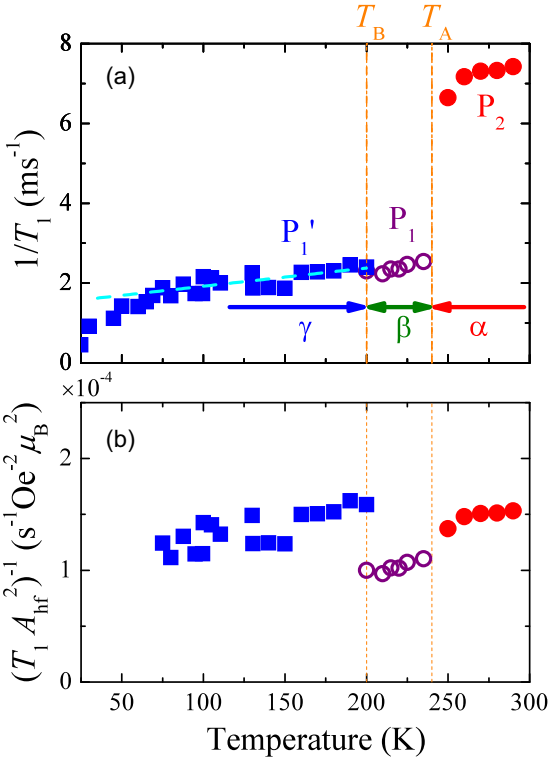

FIG. 7. (Color online) (a) Temperature dependence of $1/T_1$ for the P_1', P_1, and P_2 sites. The dotted line in the γ phase is a least linear fit to the data for $85 < T < 200$ K. (b) The plot of $(T_1 A_{hf}^2)^{-1}$ vs T estimated using the data in Fig. 7(a) and Table I.

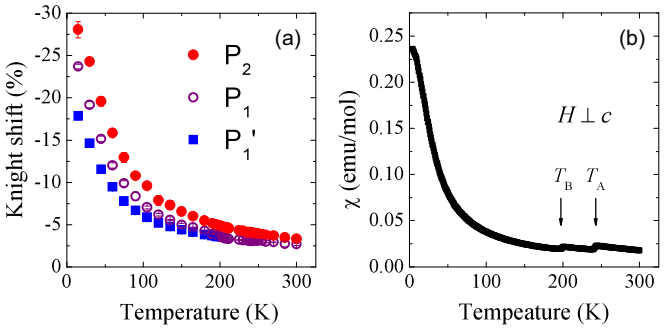

FIG. 8. (Color online) Temperature dependencies of (a) the Knight shift K for the P_1', P_1, and P_2 sites and (b) the susceptibility χ. χ was measured at a field of 7 T perpendicular to the c axis.

For the first term, when exchange interactions between local moments are regarded as constant,

$$(1/T_1)_f \sim S(S+1)A_{\rm hf}^2, \tag{2}$$

where S is the localized moments and $A_{\rm hf}$ is the hyperfine coupling constant [11]. The second term is in proportion to T, according to the Korringa relation. $1/T_1$ at the P_1' site decreases below ~75 K upon cooling, suggesting that the fluctuations of the local moments are suppressed by the application of magnetic fields. Here, the Zeeman interaction of the local moments ($\sim\mu_{\rm eff}H$) in the fields of $H = 10$–13 T approximately corresponds to 53–70 K.

Above ~75 K, $1/T_1$ in each phase shows weak temperature dependence, indicating that the first term of Eq. (1) is predominant over the T_1 relaxation process. We see from Eq. (2) that the value of $1/T_1$, which depends on site and phase, mainly reflects the values of $A_{\rm hf}$, as described later. $A_{\rm hf}$ for each P site in the three phases is evaluated from the plots of the Knight shift K versus susceptibility χ. The temperature dependencies of K for the P_1', P_1 and P_2 sites are shown in Fig. 8(a). The temperature dependence of χ, plotted in Fig. 8(b), was measured by applying magnetic field perpendicular to the c axis, so that the experimental condition is close to that of the NMR measurements: namely the powder sample is oriented perpendicular to the c axis in the NMR measurement, as mentioned above. The obtained K-χ plots are presented in Fig. 9. Here, we took into account the ordered

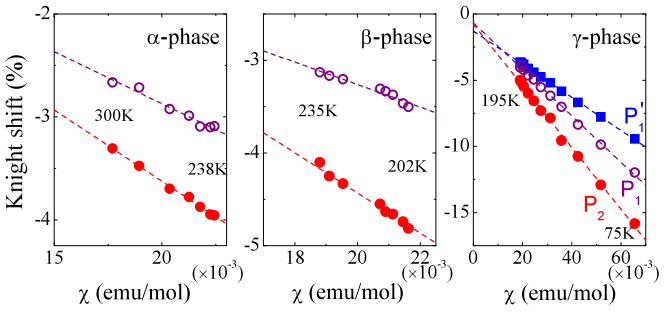

FIG. 9. (Color online) K-χ plots with temperature as an implicit parameter for the α, β, and γ phases. The solid squares, open circles, and solid circles are the data for the P_1', P_1, and P_2 sites, respectively. The dotted lines are least square fits to the data.

TABLE I. $A_{\rm hf}$ at the P_1', P_1, and P_2 sites estimated from the K-χ plots in the α, β, and γ phases shown in Fig. 9. The values for the extrinsic residual phases are given in parentheses.

	$A_{\rm hf}$ (kOe/μ_B)		
	P_1'	P_1	P_2
α	–	(-5.1 ± 0.4)	-7.0 ± 0.2
β	–	-4.8 ± 0.8	-8.6 ± 0.6
γ	-3.9 ± 0.1	(-5.4 ± 0.2)	(-7.2 ± 0.3)

structures [see in Figs. 3(b), 4(b), and 5(b)] and a reasonable assumption that only the Eu^{2+} state contributes to χ. In all cases, K and χ show a clear linear relation and $A_{\rm hf}$ is estimated by liner fits to these data. The results are summarized in Table I.

It is useful to compare the values of $A_{\rm hf}$ for the P_2 site in the α and β phases, where the P_2 site originates from the intrinsic structures of these phases. The absolute value of $A_{\rm hf}$ in the β phase is increased by about 20% compared to that in the α phase, indicating that, in the β phase, interactions between the P_2 site and the nearest neighbor Eu^{2+} layers become stronger. Since the magnitude of the Eu^{2+} local moments is supposed not to change significantly depending on phase, the present result is attributed to a decrease in the distance between the P_2 site and the Eu^{2+} layers. This is consistent with the shrinkage of the c axis which was observed by an x-ray powder diffraction experiment [5].

We plot $(T_1A_{\rm hf}^2)^{-1}$ as a function of temperature in Fig. 7(b). Here, we employed $A_{\rm hf}$ given in Table I, on the assumptions that the value and the anisotropy of $A_{\rm hf}$ do not depend on wave vector $\mathbf{q}$ and P site, respectively. The roughly close values of $(T_1A_{\rm hf}^2)^{-1}$, particularly in the α and γ phases, again suggest that the T_1 relaxation is predominantly determined by the fluctuations of the Eu^{2+} local moments and therefore the c-f hybridization is small in all the phases. Similar $4f$ states are also seen in $YbInCu_4$: $1/T_1$ is almost constant above the valence transition temperature ($T_V = 42$ K) [12,13] where the Yb valence is very close to 3+ [14]. However, an intermediate valence state abruptly develops below T_V in $YbInCu_4$ (Yb valence is ~2.84 [13]), which is different from the case of EuPtP. It is likely that the valence shift toward nonmagnetic state upon cooling, i.e., from Eu^{2+} (Yb^{3+}) to Eu^{3+} (Yb^{2+}), occurs more smoothly in the Eu compounds than in the Yb compounds. This is because the Eu^{3+} state is thermodynamically preferred at low temperatures in terms of the disappearance of local moments and smaller unit cell volume than in the Eu^{2+} state. On the other hand, the nonmagnetic Yb^{2+} state generally has larger unit cell volume than the magnetic Yb^{3+} state, which is unfavorable at low temperatures. Note that $(T_1A_{\rm hf}^2)^{-1}$ is slightly decreased in the β phase, which may be associated with the jump of the electrical resistivity along the c axis in this phase [15]. A decrease in the conductivity leads to a reduction of the minor contribution $(1/T_1)_c$ in Eq. (1).

Regarding the mechanism of the transitions, one can exclude the possibility of magnetic origin from the present studies, since we did not observe any development of magnetic correlations as approaching T_A and T_B (see Fig. 7).

Although we could not obtain crucial information to clarify the mechanism of the valence shift between integer values in EuPtP, we have detected some peculiar features of the β phase as mentioned above. Namely, in the β phase, the enhancement of $A_{\rm hf}$ and the reduction in $(T_1 A_{\rm hf}^2)^{-1}$ at the P_2 site may associated with the structural deformation and the metal-insulator like transition, respectively. These remind us characteristic features of a charge-density wave transition, and therefore the appearance of the β phase might be related to Fermi surface properties.

IV. CONCLUSIONS

We have carried out ^{31}P-NMR measurements on EuPtP. From the measurements of NMR spectrum, ordered structures and valence states in the α, β, and γ phases are presented, which explain the observed resonance lines very well. No indication of the valence fluctuations was found in the α phase. Mean Eu valences estimated from the present study are in good agreement with values determined by XAS measurements. From T_1 measurements, Eu moments were found to be in well localized state in all the phases, indicating small c-f hybridizations. We did not obtained any evidence for the development of magnetic correlations around the transition temperatures. On the other hand, we observed anomalies associated with the lattice contraction and the metal-insulator like transition at $T_{\rm A}$. These results indicate that the appearance of the β phase is not of magnetic origin, but it is purely electric or possibly associated with the Fermi surface properties.

ACKNOWLEDGMENTS

We thank K. Mimura, T. Inami, H. Harima, and H. Ikeda for valuable discussions. This work was supported by KAKENHI (Grants No. 24540349 and No. 30397666) from Japan Society for the Promotion of Science (JSPS) and a Grant-in-Aid for Scientific Research on Innovative Areas "Heavy Electrons" (No. 21102522) from the Ministry of Education, Culture, Sports, Science and Technology (MEXT) of Japan. One of the authors (G.P.) was supported by JSPS KAKENHI (No. 09F09036).

[1] For a review, see J. M. Lawrence, P. S. Riseborough, and R. D. Parks, Rep. Prog. Phys. **44**, 1 (1981).
[2] I. Felner and I. Nowik, Phys. Rev. B **33**, 617 (1986).
[3] I. Felner, I. Nowik, D. Vaknin, U. Potzel, J. Moser, G. M. Kalvius, G. Wortmann, G. Schmiester, G. Hilscher, E. Gratz, C. Schmitzer, N. Pillmayr, K. G. Prasad, H. de Waard, and H. Pinto, Phys. Rev. B **35**, 6956 (1987).
[4] For example, A. Mitsuda, S. Hamano, N. Araoka, H. Yayama, and H. Wada, J. Phys. Soc. Jpn. **81**, 023709 (2012), and references therein.
[5] N. Lossau, H. Kierspel, J. Langen, W. Schlabitz, D. Wohlleben, A. Mewis, and Ch. Sauer, Z. Phys. B **74**, 227 (1989).
[6] A. Mitsuda, T. Okuma, K. Sato, K. Suga, Y. Narumi, K. Kindo, and H. Wada, J. Phys.: Condens. Matter **22**, 226003 (2010).
[7] N. Lossau, H. Kierspel, G. Michels, F. Oster, W. Schlabitz, D. Wohlleben, Chr. Sauer, and A. Mewis, Z. Phys. B **77**, 393 (1989).
[8] G. Michels, C. Huhnt, W. Scharbrodt, W. Schlabitz, E. Holland-Moritz, M. M. Abd-Elmeguid, H. Micklitz, D. Johrendt, V. Keimes, and A. Mewis, Z. Phys. B **98**, 75 (1995).
[9] T. Inami, S. Michimura, A. Mitsuda, and H. Wada, Phys. Rev. B **82**, 195133 (2010).
[10] A. Mitsuda, T. Okuma, H. Wada, K. Sato, and K. Kindo, J. Phys.: Conf. Ser. **200**, 012119 (2010).
[11] T. Moriya, Prog. Theor. Phys. **16**, 23 (1956).
[12] H. Nakamura, K. Nakajima, Y. Kitaoka, K. Asayama, K. Yoshimura, and T. Nitta, J. Phys. Soc. Jpn. **59**, 28 (1990).
[13] T. Koyama, M. Nakamura, T. Mito, S. Wada, and J. L. Sarrao, Phys. Rev. B **71**, 184437 (2005).
[14] S. Suga, A. Sekiyama, S. Imada, J. Yamaguchi, A. Shigemoto, A. Irizawa, K. Yoshimura, M. Yabashi, K. Tamasaku, A. Higashiya, and T. Ishikawa, J. Phys. Soc. Jpn. **78**, 074704 (2009).
[15] A. Nowack, J. Klug, N. Lossau, and A. Mewis, Z. Phys. B **77**, 381 (1989).